American Mineralogist, Volume 76, pages 647–652, 1991

The crystal structure of amesite from Mount Sobotka: A nonstandard polytype

ANDRZEJ WIEWIÓRA
Institute of Geological Sciences, Polish Academy of Sciences, 02-089 Warsaw, Poland
JOSÉ A. RAUSELL-COLOM*
Instituto de Ciencia de Materiales CSIC, Serrano 115 dupl., 28006 Madrid, Spain
TERESA GARCÍA-GONZÁLEZ
Instituto de Edafología CSIC, Serrano 115 dupl., 28006 Madrid, Spain

ABSTRACT

The crystal structure of a violet phyllosilicate from the serpentinite massif of the Sobotka Mountains, lower Silesia, Poland, identified as amesite by powder diffractometry, wet chemical analysis, and IR absorption spectrometry, has been determined by single-crystal X-ray diffraction methods. The mineral has a composition close to that of the ideal end-member amesite, but with significant amounts of Cr, Fe^{2+}, and Ni. The formula is $^{[6]}(Mg_{3.80}Al_{1.75}Cr_{0.29}Fe_{0.05}Ni_{0.02}\square_{0.09})^{[4]}(Si_{2.15}Al_{1.85})O_{10}(OH)_8$.

Unit-cell dimensions obtained by least-squares refinement of 25 low- to medium-angle reflections with an automated single-crystal diffractometer gave a triclinic unit cell with parameters $a = 5.31(1)$ Å, $b = 9.212(2)$ Å, $c = 14.401(7)$ Å, $\alpha = 102.11(3)°$, $\beta = 90.2(1)°$, $\gamma = 90.1(1)°$, with two serpentine-type layers per unit cell.

The structure has been refined to an agreement factor $R = 0.061$, demonstrating the existence of ordering of cations in the tetrahedral sheet, also implying ordering of cations in the octahedral sheet. Two stacking modes occur in alternate pairs of layers, one due to a 180° rotation with no shift of neighboring layers, resulting in a change of the octahedral cation configuration, and another due to 180° rotation plus translation of $-\mathbf{b}/3$. The structure does not conform to any of the accepted standard or regular polytypes for the serpentine-like minerals.

INTRODUCTION

Amesite occurs with "sheridanite," a variety of chlorite, in vesicles in rock fragments in the soils derived from a serpentinite at Mount Sobotka, lower Silesia, Poland, as violet platy crystals forming hexagonal prisms elongated parallel to [001]. Crystals cleave in plates to thicknesses of 0.1 mm and diameters of 0.5–2 mm. Wet chemical analysis, X-ray powder diffraction patterns and infrared (IR) spectra showed the mineral to be amesite.

A powder diffraction pattern of Mount Sobotka amesite, recorded in the transmission mode with $\theta,2\theta$ coupling (Wiewióra, 1984; Wiewióra and Weiss, 1985) showed only the strongest 001 and 201 diffraction peaks; they could be indexed with an orthohexagonal unit cell of dimensions $a = 5.31$ Å, $b = 9.21$ Å, $c = 14.07$ Å, similar to that of $2H_2$ amesite (e.g., Hall and Bailey, 1979; Anderson and Bailey, 1981). However, an overexposed powder pattern obtained with a Gandolfi camera showed three very weak reflections not observed in the powder diffraction pattern with $d = 4.21$ Å, 4.03 Å, and 3.66 Å, respectively. These reflections cannot be indexed with the above unit cell. Furthermore, the characteristic reflections of the $2H_2$ polytype were not observed in the sample from Mount Sobotka. Thus, the crystal structure appears to differ from previously reported $2H_2$ amesite (Hall and Bailey, 1979; Anderson and Bailey, 1981). This paper shows, by single-crystal X-ray analysis, that this material does not conform to any standard serpentine polytype and represents a two-layer polytype with nonstandard shifts of 1:1 layers.

EXPERIMENTAL

On examination with a polarizing microscope, most of the flakes of the amesite were found to consist of highly polysynthetic twinned crystals not suitable for structure determination by single-crystal methods. Eventually, a few flakes were found that showed sharp, homogeneous extinction under crossed nicols. The best of them was used for the X-ray diffraction measurements.

Other flakes of amesite were isolated from the accompanying sheridanite and were used for wet chemical analysis (Table 1), resulting in a structural formula of $^{[6]}(Mg_{3.80}Al_{1.75}Cr_{0.29}Fe_{0.05}Ni_{0.02}\square_{0.09})^{[4]}(Si_{2.15}Al_{1.85})O_{10}(OH)_8$.

The composition deviates from the ideal end-member by having less tehahedral Al and some octahedral vacancies □, in addition to Cr, Ni, and Fe. The Fe^{2+}/Fe^{3+} ratio

* Present address: NATO Scientific Affairs Division, Room AA313, Brussels B1110, Belgium.

0003–004X/91/0304–0647$02.00

Table 1. Chemical analytical data for amesite from Mount Sobotka

Component	Wt%
SiO_2	23.00
Al_2O_3	32.70
Cr_2O_3	3.90
MgO	27.30
FeO	0.60
NiO	0.31
MnO	0.007
H_2O^+	13.00
Total	100.817

has not been determined, and all Fe is assumed to be divalent by analogy to amesite from Saranovskoye (Anderson and Bailey, 1981).

X-ray diffraction measurements

A single crystal of amesite was mounted on a CAD4 diffractometer equipped with graphite-monochromated Mo$K\alpha$ radiation. Unit-cell parameters were obtained by least-squares refinement using 25 reflections (θ to 25°) based on a C-centered lattice, space group $C1$. The refined values are a = 5.31(1) Å, b = 9.212(2) Å, c = 14.401(7) Å, α = 102.11(3)°, β = 90.2(1)°, γ = 90.1(1)°.

An $\omega/2\theta$ scan mode and a time of 2 min per reflection (scan speed 5°/min; receiving slit 2° + 0.34 tan θ) were used to measure 1992 independent reflections in four octants up to θ = 30°. Of these, 1915 were considered as observed using the relation $I > 3\sigma(I)$, and they were utilized in subsequent calculations. Two standard reflections were monitored every 100 measurements, and they showed no significant intensity variations. Intensities were corrected for Lp efects.

Structure solution and refinement

The Patterson function was interpreted using the model of T and M atoms of the first layer in amesite $2H_2$ (Anderson and Bailey, 1981). Vectors at $\langle u,v,\frac{1}{2}\rangle$ of types T-T and M-M between atoms in contiguous layers clearly indicated a displacement of **a**/2 of the second layer as the main difference with respect to the structure of $2H_2$ amesite. An electron density map using T(1), T(2), M(1), M(2), and M(3) atoms, as for amesite $2H_2$, showed the T and M atomic positions of the present structure. Successive electron-density maps revealed the positions of the remaining non-H atoms of the structure.

Scattering factors for neutral atoms were taken from the *International Tables for X-ray Crystallography,* Volume 4 (1974). Most calculations were performed using the XRAY76 system (Stewart et al., 1976) of crystallographic programs running on a VAX 11/750 computer. After several cycles of least-squares refinement using unit weights, the conventional R index was reduced to 15%. At this point, an absorption correction was performed using the method described by Walker and Stuart (1983), leading to minimum and maximum absorption corrections of 0.635 and 1.490, respectively. An analysis of the weights showed no significant trends in ΔF vs. $\langle F_{obs}\rangle$ and

Table 2. Atomic parameters for amesite

	Thermal parameters as $U_{eq} = \frac{1}{3}\left[\sum_i\sum_j U_{ij}a_i^*a_j^*a_i\cdot a_j\right]10^3$				Anisotropic thermal parameters as $\exp\left[-2\pi^2\sum_i\sum_j U_{ij}h_ih_ja_i^*a_j^*\right]10^3$					
Atom	x	y	z	Ueq	U_{11}	U_{22}	U_{33}	U_{12}	U_{13}	U_{23}
T(1)	0	0	0.0400	8(1)	7(1)	6(1)	12(1)	3(1)	−2(1)	3(1)
T(2)	0.0111(9)	0.3394(5)	0.0361(4)	10(1)	6(1)	7(1)	18(2)	1(1)	1(1)	4(1)
T(11)	0.5121(6)	−0.0003(3)	0.5393(2)	10(1)	8(1)	7(1)	15(1)	−1(1)	1(1)	2(1)
T(22)	0.0267(10)	0.1693(6)	0.5356(4)	12(1)	10(2)	10(1)	15(2)	2(1)	−2(1)	4(1)
M(1)	0.1667(12)	0.2377(7)	0.2341(5)	11(1)	10(2)	3(2)	19(2)	0(1)	−2(2)	5(2)
M(2)	0.6679(12)	0.0703(7)	0.2337(5)	10(1)	9(2)	4(2)	18(2)	2(1)	0(2)	5(2)
M(3)	0.6661(15)	0.4065(9)	0.2326(6)	11(2)	8(2)	11(2)	14(3)	−2(2)	0(2)	5(2)
M(11)	0.8429(13)	0.4034(7)	0.7326(5)	12(1)	13(2)	9(2)	13(2)	2(2)	2(2)	1(2)
M(22)	0.8415(13)	0.0711(7)	0.7337(5)	13(1)	11(2)	11(2)	14(2)	1(2)	1(2)	1(2)
M(33)	0.3397(16)	0.2360(9)	0.7331(6)	17(2)	15(2)	22(2)	11(3)	−3(2)	0(2)	−1(2)
O(1)	−0.0046(12)	0.0433(7)	0.1563(5)	10(2)	5(2)	8(3)	17(3)	−1(2)	1(2)	2(2)
O(2)	−0.0169(13)	0.3792(7)	0.1585(5)	9(2)	8(3)	6(3)	15(3)	0(2)	−1(2)	4(2)
O(3)	0.0665(15)	0.1541(8)	0.0035(6)	20(2)	24(4)	9(3)	30(4)	5(3)	3(3)	8(3)
O(4)	0.7221(16)	−0.0384(9)	−0.0065(6)	20(2)	28(4)	15(3)	19(4)	−5(3)	−2(3)	10(3)
O(5)	0.7201(17)	0.3841(8)	0.0027(6)	24(2)	38(5)	7(3)	26(4)	14(3)	−1(3)	3(3)
O(11)	0.5058(13)	0.0435(8)	0.6605(6)	13(2)	7(3)	8(3)	24(4)	3(2)	3(2)	3(2)
O(22)	0.0197(12)	0.2097(7)	0.6586(5)	12(2)	8(3)	8(3)	19(3)	5(2)	3(2)	2(2)
O(33)	0.7996(16)	0.0326(9)	0.5092(7)	24(2)	20(4)	16(4)	34(5)	−5(3)	8(3)	0(3)
O(44)	0.9269(16)	0.3292(10)	0.4978(8)	33(3)	15(4)	19(4)	58(6)	−7(3)	2(4)	−4(4)
O(55)	0.2951(16)	0.0965(8)	0.4948(7)	24(2)	27(4)	11(3)	35(5)	−1(3)	2(3)	7(3)
OH(1)	0.4908(12)	0.2131(7)	0.1595(5)	10(2)	5(2)	5(3)	18(3)	0(2)	1(2)	3(2)
OH(2)	0.3170(15)	0.0940(9)	0.3060(6)	15(2)	13(3)	8(3)	25(4)	0(2)	−5(3)	4(3)
OH(3)	0.3320(14)	0.4271(8)	0.3040(6)	15(2)	8(3)	8(3)	31(4)	1(2)	−2(3)	6(3)
OH(4)	0.8196(15)	0.2636(9)	0.3051(7)	17(2)	13(3)	8(3)	29(4)	−1(2)	−2(3)	4(3)
OH(11)	0.5099(13)	0.3792(8)	0.6595(6)	16(2)	7(3)	12(3)	25(4)	0(2)	4(2)	−3(3)
OH(22)	0.1851(13)	0.4270(8)	0.8063(6)	12(2)	8(3)	7(3)	22(4)	−2(2)	−1(3)	10(3)
OH(33)	0.1919(13)	0.0983(8)	0.8057(6)	10(2)	9(3)	5(3)	20(4)	2(2)	−2(3)	9(3)
OH(44)	0.6850(14)	0.2639(8)	0.8039(6)	14(2)	12(3)	6(3)	25(4)	0(2)	0(3)	7(3)

TABLE 3. Calculated bond lengths (Å)

	to T(1)		to T(2)		to T(11)		to T(22)
O(1)	1.64	O(2)	1.73	O(11)	1.71	O(22)	1.73
O(3)	1.65	O(3)	1.70	O(33)	1.63	O(33)	1.73
O(4)	1.63	O(4)	1.79	O(44)	1.62	O(44)	1.76
O(5)	1.60	O(5)	1.69	O(55)	1.67	O(55)	1.63
Mean	1.63	Mean	1.73	Mean	1.66	Mean	1.71
	in T(1)			**in T(2)**			
O(1)-O(3)	2.64		O(2)-O(3)	2.75			
-O(4)	2.72		-O(4)	2.93			
-O(5)	2.67		-O(5)	2.65			
O(3)-O(4)	2.53		O(3)-O(4)	2.98			
-O(5)	2.62		-O(5)	2.81			
O(4)-O(5)	2.75		O(4)-O(5)	2.77			
Mean	2.66		Mean	2.82			
	in T(11)			**in T(22)**			
O(11)-O(33)	2.67		O(22)-O(33)	2.68			
-O(44)	2.76		-O(44)	2.81			
-O(55)	2.77		-O(55)	2.79			
O(33)-O(44)	2.70		O(33)-O(44)	2.85			
-O(55)	2.76		-O(55)	2.71			
O(44)-O(55)	2.57		O(44)-O(55)	2.90			
Mean	2.71		Mean	2.79			
			to M(1)		**to M(2)**		**to M(3)**
O(1)			2.11		2.06		2.05
O(2)			2.10		2.10		1.98
OH(1)			2.02		2.08		2.09
OH(2)			2.00		2.13		1.99
OH(3)			2.02		2.02		2.04
OH(4)			2.10		2.02		2.02
Mean			2.06		2.07		2.03
			to M(11)		**to M(22)**		**to M(33)**
O(11)			2.01		2.06		2.06
O(22)			2.10		2.07		1.99
OH(11)			2.04		2.07		2.07
OH(22)			2.09		2.03		2.03
OH(33)			2.05		2.12		1.97
OH(44)			1.99		2.03		2.08
Mean			2.05		2.06		2.03
				Interlayer contacts			
OH(2). . .O(55)			2.72	OH(22). . .O(4)			2.65
OH(3). . .O(33)			2.92	OH(33). . .O(3)			2.87
OH(4). . .O(44)			2.77	OH(44). . .O(5)			2.85
			in M(1)		**in M(2)**		**in M(3)**
O(1)-O(2)			3.09		3.11		3.00
-OH(1)			3.05		3.10		3.05
O(2)-OH(1)			3.10		3.07		3.03
OH(2)-OH(3)			3.08		3.14		2.99
-OH(4)			3.07		3.09		3.04
OH(3)-OH(4)			3.11		3.10		3.00
Mean unshared			3.08		3.10		3.02
O(1)-OH(2)			2.70		—		2.70
-OH(3)			—		2.72		2.72
-OH(4)			2.79		2.79		—
O(2)-OH(2)			—		2.73		2.73
-OH(3)			2.76		2.76		—
-OH(4)			2.70		—		2.70
OH(1)-OH(2)			2.74		2.74		—
-OH(3)			2.69		—		2.69
-OH(4)			—		2.69		2.69
Mean shared			2.73		2.74		2.71
			in M(11)		**in M(22)**		**in M(33)**
O(11)-O(22)			3.07		3.13		3.01
-OH(11)			3.03		3.07		3.10
O(22)-OH(11)			3.13		3.05		3.03
OH(22)-OH(33)			3.06		3.12		3.03
-OH(44)			3.05		3.11		3.05
OH(33)-OH(44)			3.08		3.10		3.03
Mean unshared			3.07		3.10		3.04
O(11)-OH(22)			2.72		2.72		—
-OH(33)			2.64		—		2.64
-OH(44)			—		2.74		2.74
O(22)-OH(22)			2.74		—		2.74
-OH(33)			—		2.70		2.70
-OH(44)			2.72		2.72		—
OH(11)-OH(22)			—		2.70		2.70
-OH(33)			2.76		2.76		—
-OH(44)			2.69		—		2.69
Mean shared			2.71		2.72		2.70

Note: All standard deviations = 0.01 Å.

Table 5. Characteristics of amesite structures

	Tetrahedral sheet								Octahedral sheet						
Layer	*P*	*d*(T-O)	*d*(O-O)	*da*/*db**	*t*	Δ*z*	α°	τ°	*P*	*d*(M-A)	*d*(A-A)	ψ°	δ°	*t*	Ref.
Lower	T1	1.639	2.676	1.036	2.265	0.082	13.6	109.4	M1	2.096	2.957	61.1	5.78	2.023	
	T2	1.729	2.823	1.026				108.6	M2	2.087	2.944	61.0	6.23		
									M3	1.946	2.749	58.6	0.45		1
Upper	T11	1.725	2.816	1.003	2.261	0.078	14.5	109.0	M11	1.947	2.750	58.7	0.45	2.023	
	T22	1.649	2.693	1.039				109.2	M22	2.096	2.956	61.1	6.15		
									M33	2.087	2.942	61.0	5.69		
Lower	T1	1.629	2.661	1.019	2.258	0.028	14.7	109.9	M1	2.056	2.900	60.6	2.35	2.016	
	T2	1.740	2.841	0.998				109.2	M2	2.000	2.823	59.7	0.02		
									M3	2.056	2.900	60.6	2.36		2
Upper	T11	1.630	2.662	1.017	2.258	0.074	14.7	109.9	M11	2.085	2.940	61.1	5.92	2.017	
	T22	1.740	2.841	0.999				109.2	M22	1.944	2.746	58.8	0.11		
									M33	2.088	2.944	61.1	5.81		
Lower	T1	1.629	2.654	1.008	2.228	0.141	13.8	110.2	M1	2.059	2.906	59.8	1.78	2.070	
	T2	1.727	2.815	1.002				106.9	M2	2.069	2.919	60.0	1.38		
									M3	2.027	2.862	59.3	0.38		3
Upper	T11	1.655	2.704	1.043	2.237	0.203	14.0	109.4	M11	2.047	2.890	59.9	1.11	2.052	
	T22	1.713	2.795	1.014				106.8	M22	2.062	2.910	60.2	0.77		
									M33	2.033	2.870	59.7	0.37		

Note: *P* = position; *d*(T-O) = average distance between central cation and anions; *d*(A-A) and *d*(O-O) = average distance between anions; *t* = layer thickness; Δ*z* = corrugation; α = angle of ditrigonalization; τ = tetrahedral angle; ψ = octahedral angle; δ = counter rotation angle; 1 = Hall and Bailey (1979); 2 = Anderson and Bailey (1981); 3 = this work; $t_t = (z_a - z_b) \cdot d_{001}$; $t_{oct} = (z_{OH} - z_{O,OH}) \cdot d_{001}$; $\Delta z = (z_{b(max)} - z_{b(min)}) \cdot d_{001}$; $\alpha = 0.5\,(120° - \text{mean Ob-Ob-Ob angle})$; $\psi = \cos^{-1}[t_{oct}/2d(\text{M-A})]$; $\delta = |(\epsilon_1 + \epsilon_3 + \epsilon_5)/3 - 60| = |(\epsilon_2 + \epsilon_4 + \epsilon_6)/3 - 60|$ (Weiss et al., 1985).

* The a = apical; b = basal.

ΔF vs. $\langle \sin\theta/\lambda \rangle$; therefore, the unit-weighting scheme was maintained. Anisotropic thermal parameters were introduced, and convergence was achieved at $R = 6.1\%$ and $R_w = 6.6\%$. Atomic positions for the H atoms were not located in the difference map.

The final atomic coordinates, thermal parameters, and bond lengths are given in Tables 2 and 3. A list of observed and calculated structure amplitudes is in Table 4.[1]

Discussion

Bond lengths (Table 3) reveal evidence of ordering of cations in tetrahedral and octahedral cation sites. Ordering in amesite was previously reported in the structure refinements of $2H_2$ amesite, i.e., Si and Al alternating in contiguous tetrahedra and Al preferentially located in one of the three M octahedral sites. In Saranovskoye amesite, Anderson and Bailey (1981) found the smaller M(2) and M(22) octahedra of adjacent layers to be Al-rich, whereas in Antarctica amesite (Hall and Bailey, 1979) Al is concentrated in the M(3) and M(11) sites. In both of these amesite samples, ordering was found to be substantial but incomplete, in accord with the bulk composition.

In the case of Mount Sobotka amesite, Al is concentrated in sites T(2) and T(22) of adjacent layers. Average T-O distances (Table 3) indicate Al occupancies of 0.70 for T(2) and 0.67 for T(22), smaller than the occupancies reported for the Al-rich positions in Saranovskoye amesite (0.86) and in Antarctica amesite (0.74) (Anderson and Bailey, 1981; Hall and Bailey, 1979). With respect to ordering of Al in the octahedral sheet, M-O,OH bond distances in Table 3 indicate less cation ordering than in the structures of the previously refined $2H_2$ amesite crystals. For an octahedral Al content of 0.875 Al per $O_5(OH)_4$, average M-O,OH distances are 2.03 Å for the small, Al-rich, M(3), and M(33) octahedra, and 2.05–2.07 Å for the large, Mg-rich octahedra. By comparison, distances reported for Antarctica amesite were 2.09 Å for the large Mg-rich octahedra and 1.95 Å for the small Al-rich octahedra corresponding to an octahedral Al content of 0.951 Al per $O_5(OH)_4$. Distances reported for Saranovskoye amesite were 2.056 Å and 2.085 Å for the Mg-rich octahedra and 2.000 Å for the Al-rich octahedra, the Al content being 0.943. Assuming that these variations are significant, octahedral cation occupancies cannot be determined using M-(O,OH) distances if the Al/R^{2+} ratio departs significantly from the ideal 1:2 ratio.

The interlayer H bond lengths are given in Table 3. They range from 2.62 Å to 2.92 Å. The values reported for the structures of Saranovskoye and of Antarctica amesite are slightly more uniform, ranging between 2.76 and 2.81 Å for the former and between 2.72 and 2.83 Å for the latter. However, different pairs of O and OH atoms are involved.

Features characteristic of 1:1 layer structures are given for Mount Sobotka amesite and compared with $2H_2$ structures in Table 5. Tetrahedral rotation angles, α, are similar for the three structures, as is the direction of rotation, i.e., clockwise for T(1) and T(11), anticlockwise for T(2) and T(22). In plan view (Fig. 1), basal O atoms are shifted toward the octahedral cations of the same layer, thereby approaching surface OH atoms on the adjacent layer, giving rise to shortened interlayer H bonds. Larger tetrahedral bond angles, τ, in Mount Sobotka

[1] Table 4 may be ordered as Document AM-91-454 from the Business Office, Mineralogical Society of America, 1130 Seventeenth Street NW, Suite 330, Washington, DC 20036, U.S.A. Please remit $5.00 in advance for the microfiche.

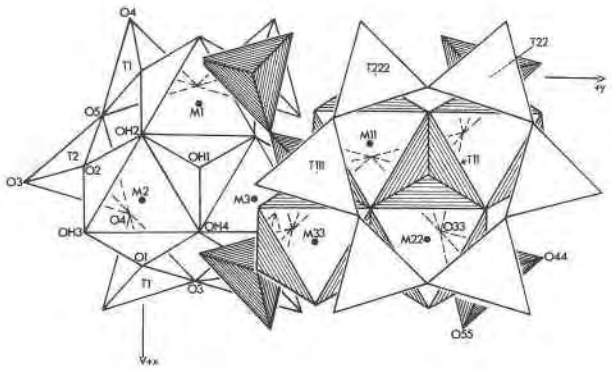

Fig. 1. View down **c*** of the structure of Mount Sobotka amesite. Layer 1 is shown on the left. Layer 2 is shown on the right, with the bases of the tetrahedra of layer 3 superimposed.

amesite result in thinner tetrahedral sheets than for the $2H_2$ amesite structures described above. Values in Table 5 assume that the inner OH atoms are part of both the tetrahedral and the octahedral sheets, so that tetrahedral sheet thicknesses for the different amesite samples are directly comparable. In contrast, values of ψ, δ, and d(A-A) for the Mount Sobotka amesite indicate smaller distortions of octahedra and, consequently, thicker octahedral sheets than for the $2H_2$ structures. Finally, the Δz values for the basal O atoms are large, and surface corrugation may affect the junction between layers by some keying together of the surfaces, as in the $2H_2$ amesite.

In the derivation of the 12 standard polytypes of 1:1 trioctahedral layer structures, Bailey (1963, 1969) showed that optimum interlayer H bonds could only be formed by three possible relative positions of adjacent layers, involving either a shift of **a**/3 along the fixed x_1, x_2, or x_3 axes of the lower layer (orthohexagonal frame of reference), or no shift of the upper layer, or shifts of $\pm$**b**/3 along the hexagonal y axes, with or without a change of octahedral cation configuration in alternating layers. It was assumed that layers had ideal hexagonal geometry and that the three layer superposition modes cannot be intermixed within the same crystal structure. For the case of alternating sets of octahedral cation configuration, only four standard polytypes with a c repeat unit of 14 Å resulted, i.e., $2M_2$ and $2Or$ if interlayer shifts are along the x axis, $2H_1$ with no shift, and $2H_2$ with a shift along the y axis. None of these polytypes has a unit cell compatible with the unit-cell parameters reported here.

When observed along the triclinic **c** axis, the layer stacking sequence of the present two-layer polytype is seen to be determined by the alternation of sets (II → I) of octahedral cation configuration, as for the $2H_1$ and $2H_2$ amesite structures, plus a shift of **a**/2 for all consecutive layers. Such a shift is apparent from the atomic coordinates of equivalent cation sites in the top and bottom layers (Table 2).

On the other hand, if layers are viewed along the direction of the **c*** axis, i.e., perpendicular to the **a**-**b** plane

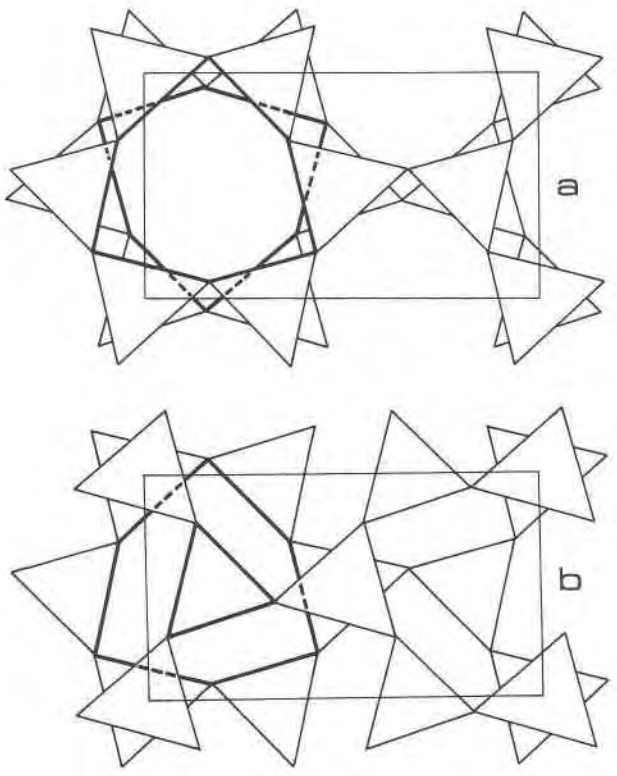

Fig. 2. Stacking modes of pairs of alternating layers. (**a**) Bases of the tetrahedra of layers 1 and 2; (**b**) bases of the tetrahedra of layers 2 and 3.

(Fig. 2), then the actual displacement vector for contiguous layers is **a**/2 − **b**/6. Such a vector does not correspond to any of the two-layer standard serpentine polytypes (Bailey, 1988). Two stacking modes result for alternating pairs of layers (Fig. 2). For the first pair (layers 1–2), the position of layer 2 relative to layer 1 is equivalent to a 180° rotation with no shift, involving a change for the octahedral cation configuration from set II to set I and leaving the centers of the ditrigonal cavities in the tetrahedral sheets of the two layers exactly superimposed. For the second pair (layers 2–3), the displacement vector again involves a change of set (I → II) for the octahedral cation configuration of layer 3, but the centers of the ditrigonal cavities of layers 2 and 3 are shifted by −**b**/3, leaving a tetrahedron of the third layer superimposed on the center of each ditrigonal ring of the second layer. For the third pair (layers 3 and 4), the stacking is identical to that for the first pair, and so on.

The intermixing of zero shift and y-axis shifts for serpentine-like layers has been studied in some detail by Hall et al. (1976). They considered all the possible six-layer stacking sequences that could be formed with these shifts and designated as the $6R_2$ polytype a model structure with regular alternation of 0 and −**b**/3 shifts plus alternation of the octahedral cation configuration. This is the six-layer equivalent of the polytype described here. A nat-

urally occurring six-layer structure with identical stacking modes (rotation, and rotation plus translation) was first reported for amesite from Saranovskoye by Steadman and Nuttall (1962).

Conclusions

The relationship between the present structure and those described as regular (or standard) polytypes by Bailey (1969, 1988) has been established as a combination of two standard polytypes. In the $2H_1$ polytype the stacking mode is due to 180° rotation of all consecutive layers, whereas in the $2H_2$ and $6R$ polytypes the stacking sequence is by $\pm\mathbf{b}/3$ translations plus 180° rotations of all consecutive layers. In the present structure the layer superposition modes of both $2H_1$ and $2H_2$ polytypes are intermixed. A displacement vector for consecutive layers of $\mathbf{a}/2 - \mathbf{b}/6$ results in a two-layer structure with a triclinic unit cell ($\alpha = 102.11°$), equivalent to a six-layer structure with an orthohexagonal cell.

Acknowledgments

Appreciation is expressed to Z. Walenczak for providing a sample of the amesite studied. This research was supported by the Dirección General de Investigatión Científica y Técnica, MEC, of Spain. The support from CICYT (project PB86-624) is gratefully acknowledged.

References cited

Anderson, C.S., and Bailey, S.W. (1981) A new cation ordering pattern in amesite-2H$_2$. American Mineralogist, 66, 185–195.

Bailey, S.W. (1963) Polymorphism of the kaolin minerals. American Mineralogist, 48, 1196–1209.

——— (1969) Polytypism of trioctahedral 1:1 layer silicates. Clays and Clay Minerals, 17, 355–371.

——— (1988) X-ray diffraction identification of the polytypes of mica, serpentine, and chlorite. Clays and Clay Minerals, 36, 193–213.

Hall, S.H., and Bailey, S.W. (1979) Cation ordering pattern in amesite. Clays and Clay Minerals, 27, 241–247.

Hall, S.H., Guggenheim, S., Moore, P., and Bailey, S.W. (1976) The structure of Unst-type 6-layer serpentines. Canadian Mineralogist, 14, 314–321.

International Tables for X-ray Crystallography (1974) Vol. IV, Kynoch Press, Birmingham, United Kingdom.

Steadman, R., and Nuttall, P.M. (1962) The crystal structure of amesite. Acta Crystallographica, 15, 510–511.

Stewart, J.M., Machin, P.A., Dickinson, C.W., Ammon, H.L., Heck, H., and Flack, H. (1976) The X-ray system. Technical Report TR-446, Computer Science Center, University of Maryland, College Park, Maryland.

Walker, N., and Stuart, D. (1983) An empirical method for correcting diffractometer data for absorption corrections. Acta Crystallographica, A39, 158–166.

Weiss, Z., Rieder, M., Chmielova, M., and Krajicek, J. (1985) Geometry of the octahedral coordination in micas: A review of refined structures. American Mineralogist, 70, 747–757.

Wiewióra, A. (1984) Rentgenowska ilosciowa analiza fazowa metoda transmisjna z korekcja orientacji dla krzemianow warstwowych. Archiwum Mineralogiczne, 40, 5–21.

Wiewióra, A., and Weiss, Z. (1985) X-ray powder transmission diffractometry determination of mica polytypes: Method and application to natural samples. Clay Minerals, 20, 231–248.

Manuscript received April 5, 1990
Manuscript accepted December 18, 1990